



DECARBURISATION OF FERRITE LATHS DURING BAINITE REACTION IN ADI

Zdzisław Ławrynowicz *, Stanisław Dymski

*University of Technology and Life Sciences in Bydgoszcz
Department of Materials Science and Engineering
Mechanical Engineering Faculty
Av. Kaliskiego 7, 85-796 Bydgoszcz, Poland
* E-mail address: lawry@utp.edu.pl*

Abstract

The paper presents an investigation of the time required for the diffusion of carbon out of supersaturated laths of ferrite into the retained austenite. Experimental measurements of volume fraction of bainitic ferrite and volume of the untransformed austenite indicate that there is a necessity of carbides precipitation from austenite. A consequence of the precipitation of cementite from austenite during austempering is that the growth of bainitic ferrite can continue to a larger extent and that the resulting microstructure is not an ausferrite, but is a mixture of bainitic ferrite, retained austenite and carbides. The carbon concentration in retained austenite demonstrates that at the end of bainite reaction the microstructure must consist of not only ausferrite but additionally precipitated carbides.

Key words: carbon diffusion, decarburisation, bainite, ductile iron ADI

1. Introduction

The development of austempered ductile iron (ADI) is a major achievement in cast iron technology. The starting material for the development of ADI is the high quality ductile or nodular cast iron. It is then subjected to an isothermal heat treatment process known as “austempering”. The attractive properties of ADI are related to its unique microstructure that consists of ferrite and high carbon austenite. Because of this microstructure, the product of austempering reaction in ductile iron is often referred to as “ausferrite” rather than bainite [1,2].

Ausferrite consists of ferrite and high carbon, stabilised austenite. If ADI is kept for long time periods, the high carbon austenite will eventually undergo transformation into bainite, the two phase ferrite and carbide ($\alpha + \text{Fe}_3\text{C}$).

During isothermal transformation, the excess carbon in the bainite partitions into the residual austenite, forcing the next plate to grow from carbon enriched austenite. The process finally ceases as the austenite carbon content reaches T_0^* value, leading to the so-called ‘incomplete reaction

* The T_0 temperature can be defined [3] such that stress free austenite and ferrite of the same composition (with respect to both the interstitial and the substitutional alloying elements) are in metastable equilibrium. Thus any displacive transformation involving a full supersaturation of carbon (i.e. bainitic ferrite would then inherit the carbon content of

phenomenon' [4]. This also explains why the degree of transformation to bainite is zero at the bainite start temperature (B_s) and increases with undercooling below B_s .

The purpose of the present paper is to demonstrate how a thermodynamic method can be used for solving a problem of the mechanism of bainite reaction in ADI and determination of the carbon concentration in the retained austenite. This should in principle enable to examine the partitioning of carbon from supersaturated ferrite laths into adjacent austenite and the carbon content in retained austenite using analytical method.

2. Material and methods

The chemical composition of the experimental ductile iron is listed in Table 1. The concentration of alloying elements in the matrix is obtained from the chemical analysis. Ductile iron blocks were produced in a commercial foundry furnace. The melt was poured into a standard Y block sand molds (ASTM A-395), which ensured sound castings. Specimens austenitised at $T_\gamma = 950^\circ\text{C}$ for 60 minutes were rapidly transferred to a salt bath at austempering temperatures 250, 300, 350 and 400°C , held for 15, 30, 60, 120 and 240 minutes, and then water-quenched to room temperature. The microstructure of the as-cast material matrix contains 40% ferrite and 60% pearlite, however graphite nodules in material is 11.5%.

After heat treatment, the samples were prepared for metallographic analysis. The samples were etched using 2% nital. Optical micrographs were taken with a Nikon camera attached to a light microscope.

Tab. 1. Chemical composition of ductile cast iron ADI, wt-%

C	Si	Mn	P	S	Mg	Cr	Ni	Mo
3.21	2.57	0.28	0.06	0.01	0.024	0.036	0.098	0.015

The X-ray investigations were performed on the specimens heat treated after a specific time of the isothermal bainite reaction at the given temperature. The total volume fraction of the retained austenite was measured from the integral intensity of the $(111)_\gamma$ and $(011)_\alpha$ peaks. The presence of high silicon content in ADI retards the formation of cementite in ferrite and austenite. The carbon concentration was calculated from measured lattice parameter of the retained austenite. The 2θ values for austenite peaks were used to calculate the d spacing with Bragg's law and then the lattice parameters. The lattice parameter of austenite (a_γ) is related to the known relationship between the parameter and the carbon concentration [5]:

$$a_\gamma \text{ (nm)} = 0.3573 + 0.0033 x_\gamma \quad (1)$$

where x_γ is the carbon concentration in austenite, in weight %.

The matrix carbon concentration, x_γ^m , of the ductile iron was also determined experimentally with Dron 1.5 diffractometer using $\text{Co } K_\alpha$ radiation on specimens austenitised at 950°C for 60 minutes and quenched to ambient temperature. It was found that after quenching the calculated carbon content in matrix is $x_\gamma^m = 1.044\% \text{C}$ and measured carbon content is $x_\gamma^m = 1.05\% \text{C}$, thus, the measured values were taken for further calculation.

the parent austenite) can occur only below the appropriate T_0 temperature. Strain energy would have effect of shifting curve to lower carbon concentration, T_0' curve [4].

3. Method of calculation of the decarburisation of supersaturated bainitic ferrite laths

The time t_d needed to decarburise the ferrite is intuitively expected to be at least comparable to that required for a lath to complete its growth. If t_d is small relative to the time required to relieve the carbon supersaturation by the precipitation of carbides within the ferrite, then upper bainite is obtained, otherwise lower bainite forms [4, 6].

Kinsman and Aaronson [7] first considered the kinetics of the partitioning of carbon from bainitic ferrite of the same composition as the parent phase. For a plate of thickness w_α the flux of carbon is defined along with a coordinate z normal to the α/γ interface, with origin at the interface and z being positive in the austenite (Fig. 1).

The method used to calculate the time of decarburising of bainitic ferrite laths is based on the hypothesis that transformation to bainite can only occur in regions of austenite where $x_\gamma \leq x_{T_0}$, where x_γ is the carbon concentration in austenite and x_{T_0} is the carbon concentration corresponding to the T_0 curve. As a lath of bainitic ferrite forms it partitions its excess carbon into the retained austenite. This creates a carbon diffusion field around the lath. Another parallel lath (of the same sheaf) which forms subsequently can only approach the original lath to a point where $x_\gamma \leq x_{T_0}$. The method assumes that the interval between lath formations is larger than the time required to decarburise each lath.

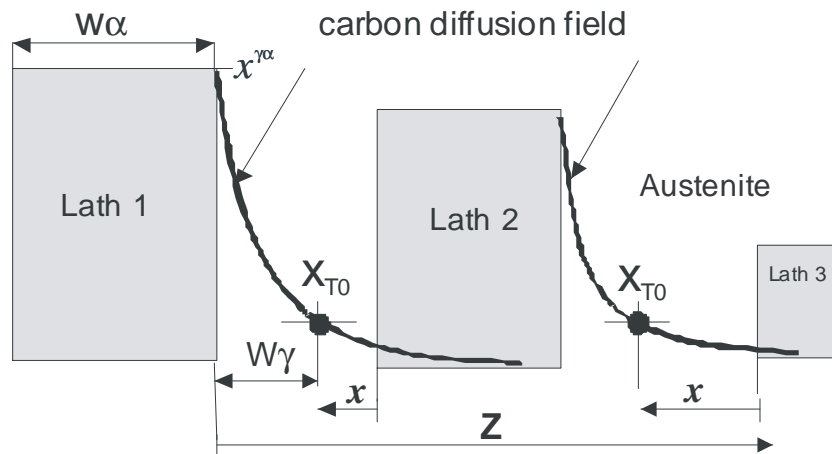


Fig. 1. Schematic diagram of method used in estimating the time of decarburising the bainitic ferrite laths. Lath 1 forms first and lath 2 and 3 and next is allowed to approach it to point where $x_\gamma \leq x_{T_0}$ (distance of this point from lath 1 is denoted w_γ). This is in fact the thickness of the retained austenite film. The mean thickness of the retained austenite films is almost tenfold thinner (0.01-0.02 μm) than the average thickness of the bainitic ferrite laths ($\sim 0.2 \mu\text{m}$).

The average carbon diffusion distances also depend on the mean spacing between the graphite nodules. Figure 2 shows a photomicrograph which contains graphite nodules with diverse distance between them, changing from about 150 to 50 μm (marked z_1 and z_2 in Fig. 2). Thus, the average distance among nodules in the examined ADI is assumed about 100 μm .

The problem is the calculation of the sum of the decarburisation times of all bainite laths existing on the coordinate connecting the nearest graphite nodules (Fig. 2).

The time needed to decarburise the ferrite matrix between the adjacent nodules of graphite t_{dz} :

$$t_{dz} = \sum_i t_{di} \quad (2)$$

where t_{di} is the time required to decarburise individual supersaturated bainitic ferrite lath of specific thickness $w_{\alpha i}$.

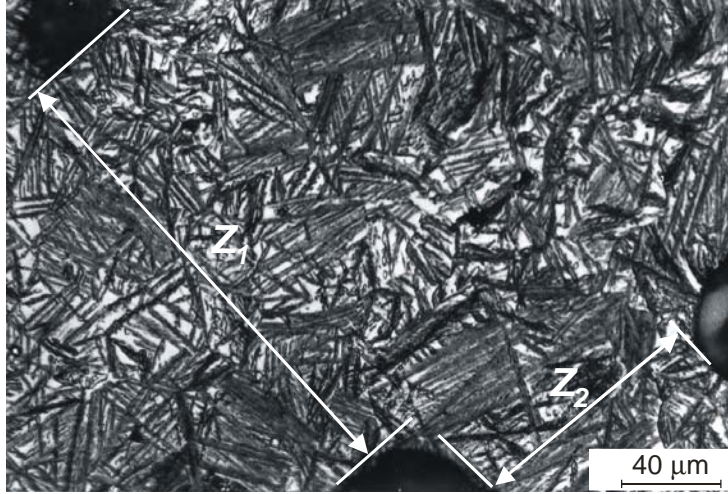


Fig. 2. Microstructure of ADI austenitised at 950 °C and austempered at 350 °C for 240 min. Etched with 2% nital

Because of the inhomogeneous distribution of carbon and other solutes in the matrix after transformation to bainite the retained austenite is enriched to a greater extent in the immediate vicinity to bainite platelets or in the region trapped between the platelets and in the eutectic cell boundary while other region contains relatively poor carbon [5, 6, 8]. The above effect can be exaggerated in ADI, since cast iron is usually extremely segregated. Martensite is usually found to be in the cell boundary which solidified last [9, 10, 11]. It indicates that the austenite in cell boundary is less enriched with carbon, and therefore is thermally unstable. From the mass balance for carbon it follows that [8]:

$$(0.5w_{\alpha})(\bar{x} - x^{\alpha\gamma}) = \int_{z=0}^{\infty} [x_{\gamma}\{z, t_d\} - \bar{x}] dz \quad (3)$$

where \bar{x} is the average mole fraction of carbon in the alloy and $x^{\alpha\gamma}$ and $x^{\gamma\alpha}$ are the paraequilibrium carbon concentration in ferrite and austenite respectively. Since the diffusion rate of carbon in austenite is slower than in ferrite, the rate of decarburisation will be determined by the diffusivity in the austenite and the concentration of carbon in austenite at the interface remains constant for times $0 < t < t_d$ after which it steadily decreases as the austenite becomes homogeneous in composition. The equation (3) corrects an error in the original treatment, the error had the effect of allowing $t_d \rightarrow 0$ as the upper integration limit $\rightarrow \infty$. The function x_{γ} is given by [8]:

$$x_{\gamma} = \bar{x} + (x^{\gamma\alpha} - \bar{x}) \operatorname{erfc}\{z / 2(Dt_d)^{0.5}\} \quad (4)$$

This assumes that for $t < t_d$, the concentration of carbon in the austenite at the interface is given by $x^{\gamma\alpha}$.

The diffusion coefficient of carbon in austenite $D\{x\}$, is very sensitive to the carbon concentration and this has to be taken into account in treating the large concentration gradients that develop in the austenite. It is clearly necessary to know $D\{x\}$ at least over a range $\bar{x} \rightarrow x^{\gamma\alpha}$, although experimental determinations of $D\{x\}$ do not extend beyond $x = 0.06$. The value of D was calculated as discussed in Ref. [12, 13]. The good approximation of the dependent diffusivity of carbon in austenite can be a weighted average diffusivity \bar{D} [14]. Taking into account carbon concentration gradients, it has been demonstrated that for most purposes a weighted average diffusivity \bar{D} can adequately represent the effective diffusivity of carbon [12-15]. Weighted average diffusivity \bar{D} is calculated by considering the carbon concentration profile in front of the moving ferrite interface as given by the following equation [12]:

$$\bar{D} = \int_{\bar{x}}^{x^{\gamma\alpha}} \frac{Ddx}{(x^{\gamma\alpha} - \bar{x})} \quad (5)$$

The calculated diffusion coefficients of carbon in austenite are listed in Table 2.

Tab. 2. The calculated diffusion coefficients of carbon in austenite $D\{x\}$ and a weighted average diffusivity \bar{D} after austenitisation at 950 °C and austempering at 400, 350, 300 and 250 °C.

Diffusion coefficients	Austempering temperature, °C			
	250	300	350	400
D [m ² /s]	0.2544×10^{-18}	0.4328×10^{-17}	0.4688×10^{-16}	0.3574×10^{-15}
\bar{D} [m ² /s]	*	*	0.5013×10^{-15}	0.1672×10^{-14}

* Diffusion calculation outside of permitted range. Siller-McLellan model fails at high carbon concentrations evaluate \bar{D} .

On carrying the integration, the time required to decarburise a supersaturated bainitic ferrite lath of thickness w_α is given by [8]:

$$t_d = \frac{w_\alpha^2 \pi (\bar{x} - x^{\alpha\gamma})^2}{16 \bar{D} (x^{\gamma\alpha} - \bar{x})} \quad (6)$$

where: \bar{x} is the average carbon concentration in the alloy, $x^{\alpha\gamma}$ and $x^{\gamma\alpha}$ are the carbon concentrations in ferrite and austenite respectively, when the two phases are in paraequilibrium.

4. The calculation of decarburisation times

For the investigated ductile cast iron ADI, our calculations show that t_d increases sharply as the thickness of the ferrite laths increases, see Table 3.

Tab. 3. Decarburisation times (t_d) in seconds of distance of 50 μm , consisted of laths with thickness: 0.1 μm ; 0.2 μm ; 0.5 μm ; 1.0 μm ; 10 μm ; 50 μm .

Ti, °C	Decarburisation times (t_d) in seconds of distance of 50 μm					
	50 μm	5×10 μm	50×1 μm	100×0.5 μm	250×0.2 μm	500×0.1 μm
400	110600	22125	2212	1128	451	225
350	234500	46905	4690	2361	950	470

The calculated times of partitioning are shown in Figure 3 for thickness of bainitic ferrite phase equal 50 μm but consisted of laths with different wideness: 0.1 μm ; 0.2 μm ; 0.5 μm ; 1.0 μm ; 10 μm and 50 μm .

The decarburisation time t_d as a function of α phase width increases with decreasing austempering temperature, because the diffusion coefficient of carbon also decreases with temperature (Table 2). The decarburisation time also increases as the thickness of the ferrite laths increases (Fig.3).

Furthermore, it is generally observed (Fig. 2) that the width of ferrite laths is highly diverse [6]. This reflect the possibility that cementite can precipitate in thicker bainite laths (when t_d is a long period of time) and in thinner laths has not during isothermal transformation. It is also consistent with the fact that upper and lower bainite often form at the same temperature in a given steel [4, 6, 16, 17, 18].

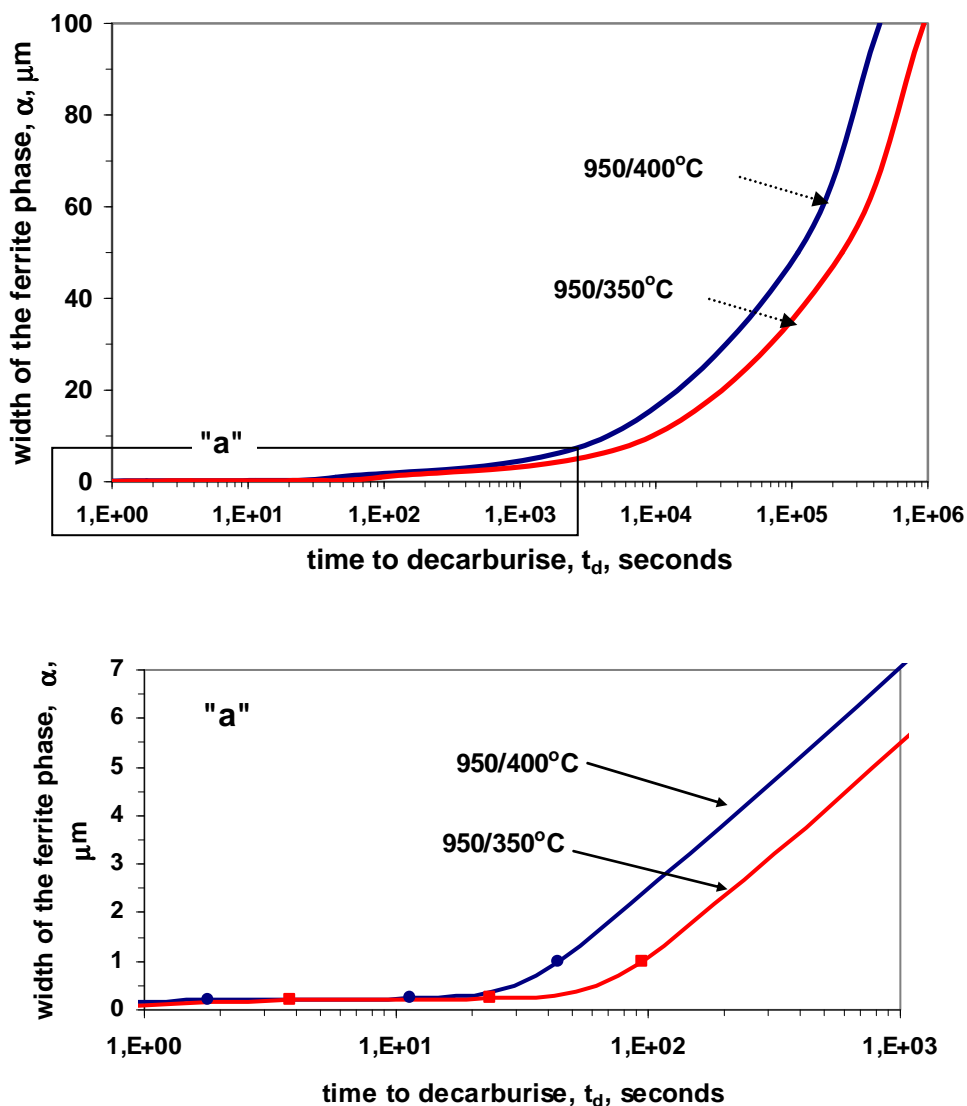


Fig. 3. The calculated times for decarburisation of ferrite phase with width of 50 μm , consisted of laths with thickness: 0.1 μm ; 0.2 μm ; 0.5 μm ; 1.0 μm ; 10 μm and 50 μm after austenitisation at 950°C. Enlarged of an area in the bottom part in Fig. 3 corresponds to the marked area "a"

5. Conclusions

The paper presents an investigation of the partitioning of carbon from supersaturated ferrite laths into adjacent austenite in ADI matrix using an analytical method. The following conclusions have been reached:

1. The extent of transformation to bainite in ductile iron, as in steels, decreases when increasing the isothermal transformation temperature towards the bainite start temperature (B_s). This is because the austenite can only transform to bainite if its carbon concentration is less than a value x_{T_0} given by the T_0 curve.
2. The bainite transformation in cast iron is essentially identical to that in steel. In steel, it has been demonstrated that the carbon concentration of the residual austenite reaches the critical value represented by the T_0 curve will render the displacive bainite reaction to cease. Therefore the carbon concentration of austenite can be estimated by the thermodynamics principles described here. Since cast iron is extremely segregated, x_γ determined by X-ray diffraction is richer than that corresponds to the T_0 curve in ADI.
3. The carbon concentration of the residual austenite increases during bainitic transformation as a consequence of the increasing volume fraction of bainitic ferrite.
4. Analytical calculations of the time required for the diffusion of carbon out of supersaturated laths of ferrite into the retained austenite indicate that there is a necessity of carbides precipitation from ferrite.
5. A consequence of the precipitation of cementite from ferrite or/and austenite during austempering is that the growth of bainitic ferrite can continue to larger extent and that the resulting microstructure is not a pure ausferrite but is a mixture of bainitic ferrite, retained austenite and carbides.

References

- [1] Chang, L. C., *Carbon content of austenite in austempered ductile iron*, pp. 35-38, Scripta Materialia 39 1998.
- [2] Pietrowski, S., *Nodular cast iron of bainitic ferrite structure with austenite or bainitic structure*, pp. 253-273, Archives of Materials Science 18 1997.
- [3] Christian, J.W., *Theory of transformations in metals and alloys*, p. 778, Oxford, Pergamon Press, 1965.
- [4] Bhadeshia, H.K.D.H., *Bainite in Steels*, pp. 1-458, Institute of Materials London 1992.
- [5] Ławrynowicz, Z., Dymski, S., *Mechanism of bainite transformation in ductile iron ADI*, Archives of Foundry Engineering 6, pp. 171-176 2006.
- [6] Ławrynowicz, Z., *Transition from upper to lower bainite in Fe-Cr-C steel*, Materials Science and Technology 20, pp. 1447-1454 2004.
- [7] Kinsman, K. R., Aaronson, H.I., *The transformation and hardenability in steels*, Climax Molybdenum Company, Ann Arbor, MI, p.39, 1967.
- [8] Bhadeshia, H.K.D.H., Christian, J.W., *Bainite in Steels*, Metallurgical Transactions 21A, pp. 767-797 1990.
- [9] Guzik, S. E., *Austempered cast iron as a modern constructional material*, Inżynieria Materiałowa 6, pp. 677-680 2003).
- [10] Ławrynowicz, Z., Dymski S., *Application of the mechanism of bainite transformation to modelling of processing window in ductile iron ADI*, Archives of Foundry Engineering 6, pp. 177-182 2006.
- [11] Kutsov, A., et al., *Formation of bainite in ductile iron*, Materials Science and Engineering A273-275, pp. 480-484 1999.

- [12] Bhadeshia, H.K.D.H., *Diffusion of carbon in austenite*, Metal Science 15, pp. 477-479 1981.
- [13] Ławrynowicz, Z., *Criticism of selected methods for diffusivity estimation of carbon in austenite*, Zeszyty Naukowe ATR nr 216, Mechanika 43, pp. 283-287 1998.
- [14] Siller, R.H., McLellan, R.B., *The Application of First Order Mixing Statistics to the Variation of the Diffusivity of Carbon in Austenite*, Metallurgical Transactions 1, pp. 985-988 1970.
- [15] Ławrynowicz, Z., *Bainitic transformation: estimation of carbon diffusivity in austenite on the basis of measured austenite film thickness*, Zeszyty Naukowe ATR nr 216, Mechanika 43, pp. 289-297 1998.
- [16] Takahashi, M., Bhadeshia, H.K.D.H., *A Model for the Microstructure of Some Advanced Bainitic Steels*, Materials Transaction, JIM, 32, pp. 689-696 1991.
- [17] Ławrynowicz, Z., *Carbon partitioning during bainite transformations in low alloy steels*, Materials Science and Technology 18, pp. 1322-1324 2002.
- [18] Ławrynowicz, Z., Barbacki, A., *Analiza mechanizmu izotermicznej przemiany bainitycznej w stali Cr-Mn-Si*. Archiwum Nauki o Materiałach 17, pp. 127-147 1996.